Longitudinal Resonant Electron Polarimetry

R. Talman, LEPP, Cornell University;
B. Roberts, University of New Mexico;
J. Grames, A. Hofler, R. Kazimi, M. Poelker, R. Suleiman;
Thomas Jefferson National Laboratory

2017 International Workshop on Polarized Sources,
Targets & Polarimetry,
Oct 16-20, 2017,
Daejeon 34051, Republic of Korea

2 Outline

Introduction
Detection apparatus
Constructive superposition of resonant excitations
Resonator parameters
Local Lenz law (LLL) approximation
Circuit analysis
Background resonator excitation by bunch charge
Frequency choice
Background rejection

3 Introduction

- An experiment to measure the polarization of an electron beam by measuring the excitation of a resonant cavity by the beam magnetization is proposed at Jefferson Lab.
- This is partly motivated by the need for non-destructive polarimetry in a frozen-spin electron beam, but the J-Lab experiment will use a longitudinally polarized linac beam.
- There are two major difficulties.
  - The Stern-Gerlach (SG) beam magnetization is very small, making it hard to detect in absolute terms
  - Even more serious is the smallness of the SG magnetization excitation, relative to imperfection-induced, direct excitation of the resonator by the beam charge.
- In principle, with ideal resonator construction and positioning, this background would vanish. But, because the electron charge is so large relative to its magnetic moment, special beam preparation and polarization modulation are required to suppress this background.

- The fundamental impediment to resonant electron polarimetry comes from the smallness of the magnetic moment divided by charge ratio of fundamental constants,

$$\frac{\mu_B/c}{e} = 1.930796 \times 10^{-13}\,\mathrm{m}; \qquad (1)$$

  except for a tiny anomalous magnetic moment correction and sign, the electron magnetic moment is equal to the Bohr magneton μ_B.
- This ratio has the dimension of length because the Stern-Gerlach force due to magnetic field acting on μ_B, is proportional to the *gradient* of the magnetic field.
- To the extent that it is "natural" for the magnitudes of E and cB to be comparable, Stern-Gerlach forces are weaker than electromagnetic forces by ratio (1). This adverse ratio needs to be overcome in order for magnetization excitation to exceed direct charge excitation.

5 Detection apparatus

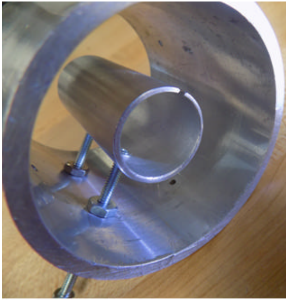

- A passive (non-destructive) high analysing power polarimetry is needed for feedback stabilization of frozen-spin storage rings—especially electrons.
- A basic resonator cell is a several centimeter long copper split-cylinder, with gap serving as the capacitance C of, for example, a 1.75 GHz LC oscillator, with inductance L provided by the conducting cylinder acting as a single turn solenoid.
- The photos show split-ring resonators (open at the ends) built and tested at UNM, resonant at 2.5 GHz, close to the design frequency.The resonator design, was introduced by Hardy and Whitehead in 1981 and has been used commonly for NMR measurements.

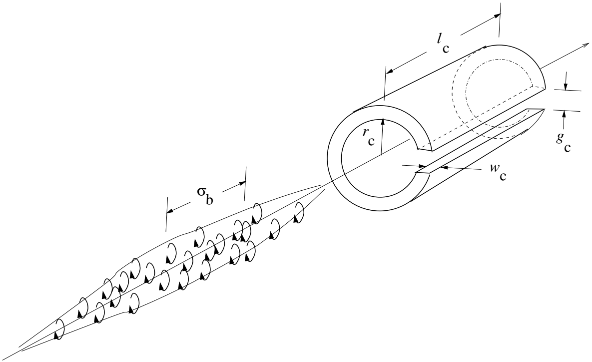

Figure: Perspective view of polarized beam bunch passing through the polarimeter. Dimensions are shown for the polarized proton bunch and the split-cylinder copper resonator. For the proposed test, using a polarized electron beam at Jefferson Lab, the bunch will actually be substantially shorter than the cylinder length, and have a beer can shape.

- Consider a single, longitudinally polarized bunch of electrons in a linac beam that passes through the split-cylinder resonator.
- The split cylinder can be regarded as a one turn solenoid.
- The bunch polarizations will toggle, bunch-to-bunch, between directly forward and directly backward.
- This is achieved by having two oppositely polarized, but otherwise identical interleaved beams, an A beam and a B beam, each having bunch repetition frequency $f_0 = 0.25\,\mathrm{GHz}$ (4 ns bunch separation).
- The resonator harmonic number relative to f_0 is an odd number in the range from 1 to 11
- This beam preparation immunizes the resonator from direct charge excitation. Irrespective of polarization, the A+B-combined bunch-charge frequencies will consist only of harmonics of $2f_0 = 0.5\,\mathrm{GHz}$, incapable of exciting the resonator(s).

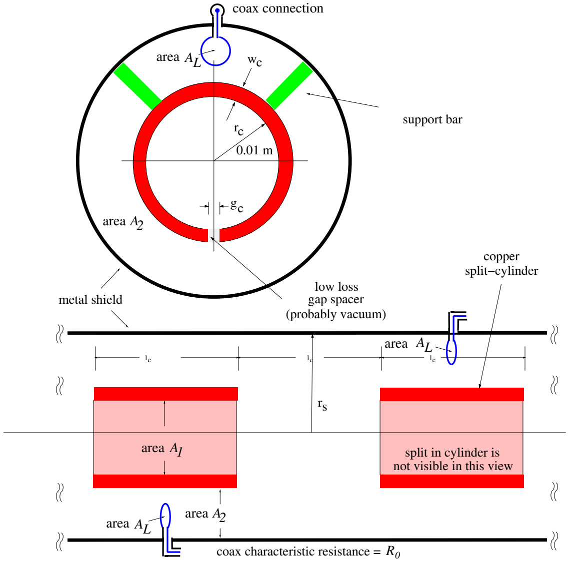

Figure: End and side views of two resonant split-cylinder polarimeter cells. Signals from individual resonators are loop-coupled out to coaxial cables and, after matched delay, added.

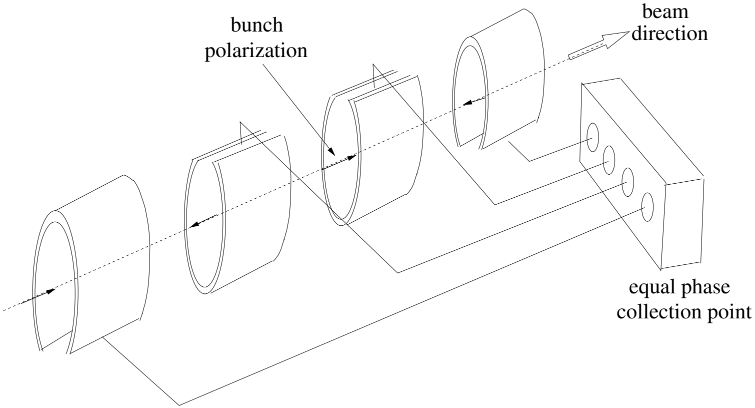

Figure: Sketch showing beam bunches passing through multiple resonators. Cable lengths are arranged so that beam polarization signals add constructively, but charge-induced, asymmetric-resonator excitations cancel.

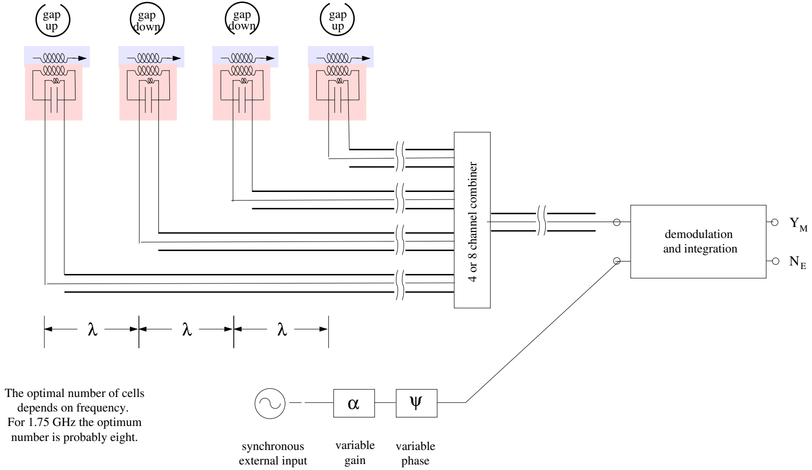

Figure: Circuit diagram for a circuit that coherently sums the signal amplitudes from four (or eight) polarimeter cells. Excitation by passing beam bunches is represented by inductive coupling. Quadrature signal separation routes in-phase signals to the Y_E ("Yes it is magnetic-induced") output, and out-of-phase, quadrature signals to the N_E ("No it is electric-induced") output. The external coherent signal processing functionality to achieve this separation is indicated schematically by the box labelled "demodulation and integration". Unfortunately the performance is not as clean as the terminal names imply.

- Four such cells, regularly arrayed along the beam, form a half-meter-long polarimeter.
- The magnetization of a longitudinally-polarized electron bunch passing through the resonators coherently excites their fundamental oscillation mode and the coherently-summed "foreground" response from all resonators measures the polarization.
- "Background" due to direct charge excitation is suppressed by arranging successive beam bunches to have alternating polarizations. This moves the beam polarization frequency away from the direct beam charge frequency.
- Charge-insensitive resonator design, modulation-induced sideband excitation, and synchronous detection, permit the magnetization foreground to be isolated from spurious, charge-induced background.

12 Constructive superposition of resonant excitations

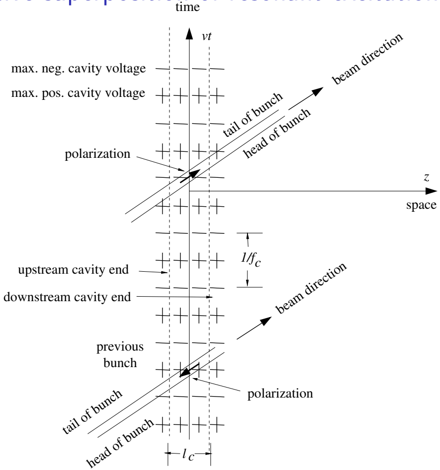

Figure: Space-time plot showing entry by the front, followed by exit from the back of one bunch, followed by the entrance and exit of the following bunch. Bunch separations and cavity length are arranged so that cavity excitations from all four beam magnetization exitations are perfectly constructive. The rows $++++$ and ---- represent equal time contours of maximum or minimum V_C, E_ϕ, dB_z/dt, or dI_C/dt, all of which are in phase..

- Treated as an LC circuit, the split cylinder inductance is L_c and the gap capacity is C_c. The highly conductive split-cylinder can be treated as a one-turn solenoid.
- For symplicity, minor corrections due to the return flux are not included in formulas given shown here
- In terms of its current I, the magnetic field B is given by

$$B = \mu_0 \frac{I}{l_c}, \tag{2}$$

- The magnetic energy W_m can be expressed in terms of B or I;

$$W_m = \frac{1}{2} \frac{B^2}{\mu_0} \pi r_c^2 l_c = \frac{1}{2} L_c I^2. \tag{3}$$

- The self-inductance is therefore

$$L_c = \mu_0 \frac{\pi r_c^2}{l_c}. \tag{4}$$

- The gap capacitance (with gap g_c reckoned for vacuum dielectric and fringing neglected) is

$$C_c = \epsilon_0 \frac{w_c l_c}{g_c}. \tag{5}$$

- Because the numerical value of C_c will be small, this formula is especially unreliable as regards its separate dependence on w_c and g_c.
- Furthermore, for low frequencies the gap would contain dielectric other than vacuum.
- Other resonator parameters, with proposed values, are given in following tables.

parameter name	parameter symbol	formula	unit	value
cylinder length	l_c		m	0.04733
cylinder radius	r_c		m	0.01
gap height	g_c		m	0.00103943
wall thickness	w_c		m	0.002
capacitance	C_c	$\epsilon_0 \frac{w_c l_c}{g_c/\epsilon_r}$	pF	0.47896
inductance	L_c	$\mu_0 \frac{\pi r_c^2}{l_c}$	nH	7.021 3
resonant freq.	f_c	$1/(2\pi\sqrt{L_c C_c})$	GHz	2.7445
resonator wavelength	λ_c	c/f_c	m	0.10923
copper resistivity	$\rho_{\rm Cu}$		ohm-m	1.68e-8
skin depth	δ_s	$\sqrt{\rho_{\rm Cu}/(\pi f_c \mu_0)}$	μm	1.2452
eff. resist.	R_c	$2\pi r_c \rho_{\rm Cu}/(\delta_s l_c)$	ohm	0.017911
unloaded. qual. factor	$\mathcal{Q}$			6760.0
effective qual. fact.	$\mathcal{Q}/h_c$			643.65
bunch frequency	$f_A = f_B = f_0$		GHz	0.2495
cavity harm. number	h_c	f_c/f_0		11
electron velocity	v_e	$c\sqrt{1-(1/2)^2}$	m/s	2.5963e8
cavity transit time	Δt	l_c/v_e	ns	0.18230
transit cycle advance	$\Delta\phi_c$	$f_c \Delta t$		0.50032
entry cycle advance		$\Delta\phi_c l_b/l_c$		0.15011
electrons per bunch	N_e			2.0013×10^6
bunch length	l_b		m	0.0142
bunch radius	r_b		m	0.002

Table: Resonator and beam parameters. The capacity has been calculated using the parallel plate formula. The true capacity is somewhat greater, and the gap g_c will have to be adjusted to tune the natural frequency. When the A and B beam bunches are symmetrically interleaved, the bunch repetition frequency (with polarization ignored) is $2f_0$.

16 Local Lenz law (LLL) approximation

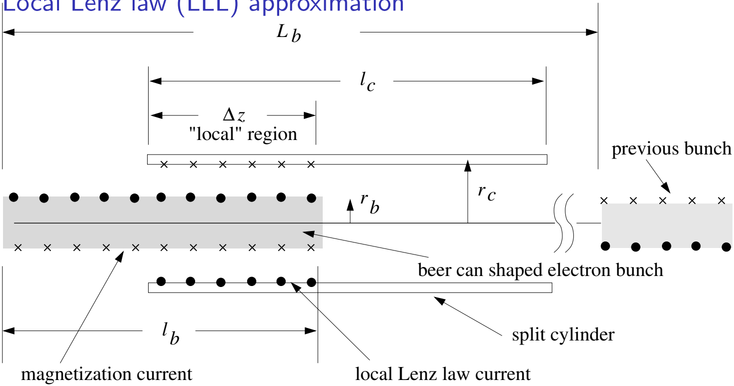

- A local Lenz law approximation for calculating the current induced in split cylinder by an electron bunch entering a split-cylinder resonator, treated as a one turn solenoid
- The electron bunch is assumed to have a beer can shape, with length l_b and radius r_b.
- Lenz's law is applied to the local overlap region of length Δz.
- Flux due to the induced Lenz law current exactly cancels the flux due to the Ampère bunch polarization current.

- The magnetization $\mathbf{M}$ within length Δz of a beam bunch (due to all electron spins in the bunch pointing, say, forward) is ascribed to azimuthal Ampẽrian current $\Delta I_b = i_b \Delta z$.
- The bunch transit time is shorter than the oscillation period of the split cylinder and the presence of the gap in the cylinder produces little suppression of the Lenz's law current
- $\Delta I_{LL} = i_{LL} \Delta z$ is the induced azimuthal current shown in the (inner skin depth) of the cylinder
- To prevent any net flux from being present locally within the section of length Δz, the flux due to the induced Lenz law current must cancel the Ampère flux.

- Let i_{LL} to be the Lenz law current per longitudinal length.
- The Lenz law magnetic field is $B_{LL} = \mu_0 i_{LL}$ and its magnet flux through the cylinder is

$$\phi_{LL} = \mu_0 \pi r_c^2 i_{LL}. \tag{6}$$

- Jackson says the magnetic field $\mathbf{B_b}$ within the polarized beam bunch is equal to $\mu_0 \mathbf{M_b}$ which is the magnetization (magnetic moment per unit volume) due to the polarized electrons.

$$B_b = \mu_0 M_B = \mu_0 \frac{N_e \mu_B}{\pi r_b^2 l_b}, \tag{7}$$

where N_e is the total number of electrons in each bunch.

- The flux through ring thickness Δz of this segment of the beam bunch is therefore

$$\phi_b = B_b \pi r_b^2 = \mu_0 \frac{N_e \mu_B}{l_b}, \tag{8}$$

- Since the Lenz law and bunch fluxes have to cancel we obtain

$$i_{LL} = -\frac{N_e \mu_B}{l_b} \frac{1}{\pi r_c^2}. \tag{9}$$

- For a bunch that is longitudinally uniform (as we are assuming) we can simply take Δz equal to bunch length l_b to obtain

$$I_{LL} = i_{LL} l_b = -\frac{N_e \mu_B}{\pi r_c^2} \tag{10}$$

- With bunch fully within the cylinder, I_{LL} “saturates” at this value.

- The bunch is short (i.e. $l_b << l_c$) so the linear build up of I_{LL} can be ascribed to a constant applied voltage V_{LL} required to satisfy Faraday's law.
- For a CEBAF I_e =160 μA, 0.5 GHz bunch frequency beam the number of electrons per bunch is approximately 2×10^6 and the Lenz law current is

$$I_{LL}^{\max} = -\frac{N_e \mu_B}{\pi r_c^2} \quad \left(\stackrel{\text{e.g.}}{=} -5.9078 \times 10^{-14}\,\mathrm{A} \right). \tag{11}$$

- The same excess charge is induced on the capacitor during the bunch exit from the cylinder at which time the resonator phase has reversed.
- The total excess charge that has flowed onto the capacitor due to the bunch passage is

$$Q_1^{\max.} \approx I_{LL}^{\text{sat.}} \frac{l_b}{v_e} \quad \left(\stackrel{\text{e.g.}}{=} -3.2312 \times 10^{-24}\,\mathrm{C.} \right). \tag{12}$$

- The meaning of the superscript "max" is that, if there were no further resonator excitations, the charge on the capacitor would oscillate between $-Q_1^{\mathrm{max.}}$ and $+Q_1^{\mathrm{max.}}$.
- Let $U_1^{\mathrm{pol.}}$ be the correspondin energy transfer. This is the "foreground" quantity that (magnified by a resonant amplitude magnification factor M_r^2) provides the polarization measure in the form of steady-state energy $U^{\mathrm{pol.}}$ stored on the capacitor;

$$\boxed{U^{\mathrm{pol.}} = \frac{1}{2}\,\frac{Q_1^{\mathrm{max.}2}}{C_c}\,M_r^2 = \Big(M_r^2 \times 1.0899 \times 10^{-35}\,\mathrm{J}\Big)} \tag{13}$$

$Q_1^{\mathrm{max.}} = 3.2312 \times 10^{-24}\,\mathrm{C}$ is the charge deposited on the resonator capacitance during a single bunch passage of a bunch with the nominal ($N_e = 2 \times 10^6$ electrons) charge.
- This equation is boxed to emphasize the importance of $U^{\mathrm{pol.}}$ both in absolute terms and for relative comparison with "background"—another excitation source, which causes spurious capacitor energy changes, will later also be boxed.

22 Circuit analysis

- In a MAPLE program the excitation is modeled using "piecewise defined" trains of pulses. Bipolar pulses modeling entry to and exit from the resonator are obtained as the difference between two, time-displaced "top hat" pulse trains

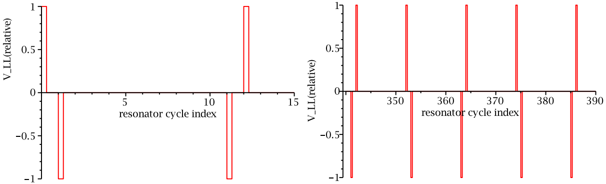

- Pulsed excitation voltage pulse are caused by successive polarized bunch passages through the resonator.
- A few initial pulses are shown on the left, some later pulses are shown on the right.
- The units of the horizontal time scale are such that, during one unit along the horizontal time axis, the natural resonator oscillation phase advances by π. The second pulse starts exactly at 1 in these units
- h_c=11 units of horizontal scale advance corresponds to a phase advance of π at the $f_A = f_B = f_0 = 0.2495\,\text{GHz}$ "same-polarization repetition frequency".

- Lumped constant representation of the split-cylinder resonator as a parallel resonant circuit is shown

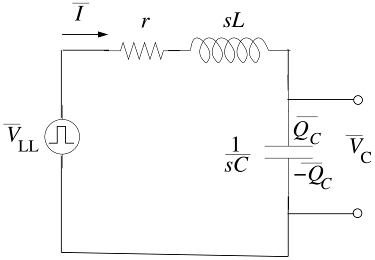

- Voltage division in this series resonant circuit produces capacitor voltage transform $\bar{V}_C(s)$;

$$\bar{V}_C(s) = \frac{1/(Cs)}{1/(Cs) + r + Ls}\,\bar{V}_{LL}(s) = \frac{\bar{V}_{LL}(s)}{1 + rs + CLs^2}. \qquad (14)$$

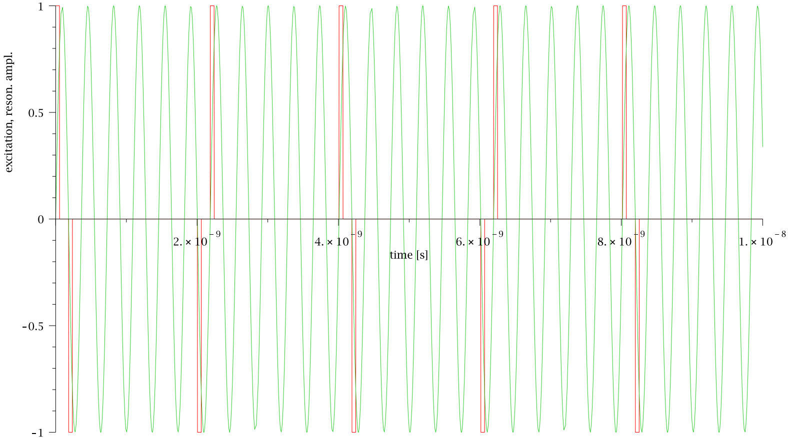

Figure: Alternating polarization excitation pulses superimposed on resonator response amplitude and plotted against time. Bunch separations are 2 ns, bunch sepraration between same polarization pulses is 4 ns. The vertical scale can represent V_C, E_ϕ, dB_z/dt, or dI_C/dt, all of which are in phase.

This comparison shows that the response is very nearly in phase with the excitation.

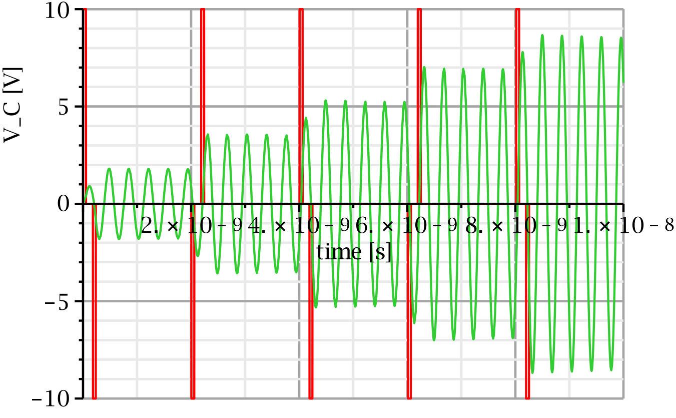

Figure: Accumulating capacitor voltage response V_C while the first five linac bunches pass the resonator. The accumulation factor relative to a single passage, is plotted.

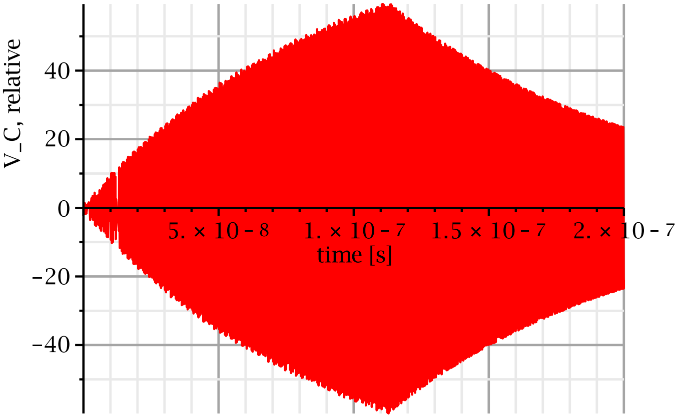

Figure: Relative resonator response to a train of beam pulse that terminates after about 110 ns. After this time the resonator rings down at roughly the same rate as the build-up. The circuit parameters are those given in Table 1, except that the resistance for the plot is $r = 10r_c$. The true response build up would be greater by a factor of 10, over a 10 times longer build-up time.

- The magnetic field shape, even at microwave frequency, is very nearly the same as the low frequency shape given by magnetostatics—uniform B_z in the interior, with return flux outside the cylinder.
- As a cylindrical waveguide open at both ends, the cylinder can also resonate at frequencies above waveguide cut-off. But, with cylinder radius r_c only 1 cm, all such resonances can be neglected—their frequencies are well above the highest value of f_c under consideration.
- To calculate the interaction of the charged bunch with the resonator we therefore need only consider the B_z, B_r and E_r components.
- even the B_z and B_r components can be neglected—they deflect the bunch but, to good approximation, they cause no energy transfer between bunch and resonator. For these reasons we can treat the orbits through the resonator as curvature-free straight lines.

- To estimate the importance of direct charge, background exitation we can assume steady-state resonator response at the level calculated for the foreground bunch magnetization response, and calculate the additional transient excitation of the resonator due to the Faraday's law electric field acting on the bunch charge.
- The saturated inductance current

$$I_L^{\mathrm{sat.}} = \frac{V_C^{\mathrm{sat.}}}{Z_c} = 3.587 \times 10^{-11}\,\mathrm{A}. \tag{15}$$

- The corresponding magnetic field is solenoidal;

$$B_c^{\mathrm{sat.}} = 0.9522 \times 10^{-15}\,\mathrm{T}. \tag{16}$$

- A very small magnetic field, oscillating at very high, 2.74 GHz frequency, with perfect regularity, which makes it significant.
- The task is to calculate the work done on a bunch caused by the corresponding Faraday's law electric field along with cavity misalignment.

29 Canted particle incidence

- The equation of a "canted" orbit path through the resonator is

$$\begin{aligned} x &= \Delta x, \\ y &= -\Delta\theta_y z = -\Delta\theta_y v_e t, \end{aligned} \tag{17}$$

- The solenoidal magnetic fields and the corresponding e.m.f. are given by

$$\begin{aligned} B_z &= B_c^{\mathrm{sat.}} \sin(\omega_c t + \psi), \\ \varphi &= \pi \Delta x^2 B_c^{\mathrm{sat.}} \sin(\omega_c t + \psi), \\ \mathrm{e.m.f.} &= -\frac{d\varphi}{dt} = -\pi \Delta x^2 B_c^{\mathrm{sat.}} \omega_c \cos(\omega_c t + \psi) \end{aligned} \tag{18}$$

- The beam bunch is subject to a Faraday's law electric force given by

$$F_y = N_e e\, E_\phi = N_e e \frac{\mathrm{e.m.f.}}{2\pi \Delta x} = -\frac{1}{2} N_e e \Delta x B_c^{\mathrm{sat.}} \omega_c \cos(\omega_c t + \psi). \tag{19}$$

- The total work done during a single bunch passage is given by

$$\boxed{W_1^{\mathrm{m.a.}} = \left(\frac{\Delta I_{\mathrm{ave}}}{2f_0} v_e B_c^{\mathrm{sat.}} \frac{1}{r_c} \right) \Big(\Delta\theta_y \Delta x \Big) = \Big(4.5 \times 10^{-20}\, \mathrm{J/m} \Big) \left(\frac{\Delta I_{\mathrm{ave}}}{I_{\mathrm{ave}}} \left|\rho\right| \Delta\theta_\perp \right).} \tag{20}$$

parameter harmonic numb.	symbol h_c	unit GHz	3	5	7	9	11
A,B bunch freq.	f_0	GHz	0.2495	0.2495	0.2495	0.2495	0.2495
resonant freq.	f_0	GHz	0.7485	1.2475	1.7465	2.2455	2.7445
dielectric			polyeth.	polyeth.	vacuum	vacuum	vacuum
rel. diel. const.	ϵ_r		2.30	2.30	1.00	1.00	1.00
numb. cells/m	N_{cell}	$\approx$ /m	4	4	4	4	4
band width	$f_c/\mathcal{Q}$	kHz	286	277	309	351	388
quality factor	$\mathcal{Q}$		2.61e+03	4.51e+03	5.65e+03	6.40e+03	7.08e+03
effective qual. fact.	$M_r = \mathcal{Q}/h_c$		8.72e+02	9.01e+02	8.07e+02	7.12e+02	6.44e+02
cyl. length	l_c	cm	17.35	10.41	7.44	5.78	4.733
cyl. radius	r_c	cm	1.0	1.0	1.0	1.0	1.000
gap height	g_c	mm	1.305	2.021	0.709	1.171	1.750
wall thickness	w_c	mm	10.0	5.0	2.0	2.0	2.0
capacitance	C_c	pF	27.076	5.245	1.859	0.874	0.479
inductance	L_c	nF	1670	3.10	4.47	5.74	7.02
skin depth	δ_s	μm	2.384	1.847	1.561	1.377	1.245
effective resistance	R_c	mΩ	2.55	5.49	9.09	13.26	17.91
cav. trans. time	Δ_t	ns	0.668	0.401	0.286	0.223	0.182
entry cycle adv.	$\Delta_t f_c l_b / l_c$		0.041	0.068	0.096	0.123	0.150
single pass energy	$U_{1,max}$	J	1.9e-37	1.0e-36	2.8e-36	6.0e-36	1.1e-35
sat. cap. volt.	$V_{C,sat}$	V	1.0e-10	5.6e-10	1.4e-09	2.6e-09	4.3e-09
sat. cap. charge	$Q_{C,sat}$	C	2.8e-21	2.9e-21	2.6e-21	2.3e-21	2.1e-21
sat. ind. curr.	$I_{L,sat}$	A	1.3e-11	2.3e-11	2.9e-11	3.2e-11	3.6e-11
signal power	P_{sig}	W	4.39e-22	4.03e-21	1.28e-20	2.72e-20	5.0e-20
therm. noise floor @1s	P_{noise}	W	4.05e-21	4.05e-21	4.05e-21	4.05e-21	4.05e-21
signal/noise at 1 s	$\log_{10}(P_{sig}/P_{noise})$	db	-9.65	-0.01	4.99	8.27	10.88
signal/noise at 100 s	" + 20	db	10.35	19.99	24.99	28.27	30.88

31 Background rejection

misalignment	misalignment factor formula	installation specification	operational improvement factor	background reduction factor
beam position	$\sqrt{\sigma_x^2+\sigma_y^2}$	$<0.001\,\mathrm{m}$	$/10^2$	1e-5
beam slope	$\sqrt{\sigma_{x'}^2+\sigma_{y'}^2}$	<0.001	$/10$	1e-4
A/B imbalance	$\Delta I_{\mathrm{ave}}/I_{\mathrm{ave}}$	<0.01	$/10$	1e-3
pol. modulate	$\mathcal{S}^{\mathrm{pol.}}$		$/10$	1e-1
slope modul	$\mathcal{S}^{\mathrm{m.a.}}$		$/10$	1e-1
noise/signal	$10^{10}\,\mathcal{S}^{\mathrm{m.a.}}\,\mathcal{S}^{\mathrm{pol.}}\,W_1^{\mathrm{m.a.}}/U^{\mathrm{pol.}}$			1e-4

- The expected saturation level resonator voltage is

$$V_C^{\mathrm{rcvr.}}=\frac{N_{\mathrm{cell}}(\mathcal{Q}/h_c)\,Q_1^{\mathrm{sat.}}}{C_c}=4.34\times10^{-9}\,\mathrm{V}. \tag{21}$$

- Accumulated over 100 s, this is expected to be 31 db above the thermal noise floor in a room temperature copper cavity.

- W. Hardy and L. Whitehead, *Split-ring resonator for use in magnetic resonance from 200-2000 MHz*, Review of Scientific Instruments, **52** (2) 213, 1981
- B. R. Johnson, *Nuclear Spin Waves in Spin-Polarized Hydrogen*, Cornell Ph.D. thesis, 1984
- Storage Ring EDM Collaboration, *A Proposal to Measure the Proton Electric Dipole Moment with* 10^{-29} *e-cm Sensitivity*, October, 2011
- J. Jackson, *Classical Electrodynamics*, 3rd edition, John Wiley, 1998
- W. Smythe, *Static and dynamic electricity*, 2nd edition, McGraw Hill, 1950
- V. Kumar, *Understanding the focusing of charged particle beams in a solenoid magnetic field*, Am. J. Phys. **77** (8) 2009
- C. Montgomery, R. Dicke, and E. Purcell, *Principles of Microwave Circuits*, McGraw-Hill, 1948

- N. Mott and H. Massey, *The Theory of Atomic Collisions*, 3rd Edition, p. 229, 1965
- Ya. S. Derbenev, *RF-resonance beam polarimeter, Part I. Fundamental concepts*, Nuclear Instruments and Methods m Physics Research A 336, 12-15, 1993
- M. Conte, et al., *The Stern-Gerlach interaction between a traveling particle and a time varying magnetic field*, arXiv:physics/0003069v1 [physics.acc-ph], 2000
- P. Cameron, et al., *An RF Resonance Polarimeter Phase I Proof of Principle Experiment*, RHIC/AP/126
- C. Tschalaer, *The Relativistic Stern-Gerlach Force*, arXiv/papers/0802/0802:0154.pdf, 2008
- C. Tschalaer, *Lorentz Transform of an Arbitrary Force Field on a Particle in its Rest Frame using the Hamilton-Lagrangian Formalism*, BIR#15-01, Bates Lab Report, 2015